June 2001

Ozone and Tracer Transport Variations in the Summer Northern Hemisphere Stratosphere

E. C. Cordero
San Jose State University, eugene.cordero@sjsu.edu

S. R. Kawa
NASA Goddard Space Flight Center, Greenbelt, Maryland

Recommended Citation
E. C. Cordero and S. R. Kawa. "Ozone and Tracer Transport Variations in the Summer Northern Hemisphere Stratosphere" *Journal of Geophysical Research: Atmospheres* (2001). doi:10.1029/2001JD900004

JOURNAL OF GEOPHYSICAL RESEARCH, VOL. 106, NO. D11, PAGES 12,227–12,239, JUNE 16, 2001

Ozone and tracer transport variations in the summer Northern Hemisphere stratosphere

E. C. Cordero

Department of Mathematics and Statistics, Monash University, Clayton, Victoria, Australia

S. R. Kawa

Atmospheric Chemistry and Dynamics Branch, NASA Goddard Space Flight Center, Greenbelt, Maryland

Abstract. Constituent observations from the Upper Atmosphere Research Satellite (UARS) in combination with estimates of the residual circulation are used to examine the transport and chemical budgets of HF, CH_4 and O_3 in the summer Northern Hemisphere. Budget calculations of HF, CH_4 and O_3 show that the transport tendency due to the residual circulation increases in magnitude and is largely opposed by eddy motions through the summer months. Ozone budget analyses show that between 100 and 31 hPa, the magnitudes of the mean circulation and eddy transport terms increase through the summer months, producing tendencies that are factors of 2 to 3 times larger than the observed ozone change in the stratosphere. Chemical loss dominates the observed ozone decrease only at the highest latitudes, poleward of about 70°N. A comparison of observations from the Total Ozone Mapping Spectrometer with UARS-calculated total ozone suggests that poleward of 50°N, between 35% and 55% of the seasonal ozone decline during the summer occurs at altitudes below 100 hPa. The overall uncertainties, associated primarily with calculations of the residual circulation and eddy transport, are relatively large, and thus prevent accurate and useful constraints on the ozone chemical rate in the lower stratosphere.

1. Introduction

The annual cycle in stratospheric ozone has been studied for many years [e.g., *Bowman and Krueger*, 1985; *Krueger*, 1989; *Perliski et al.*, 1989]. Data from the ground-based Dobson spectrophotometer network and the Total Ozone Mapping Spectrometer (TOMS) show a pronounced annual cycle in ozone in the middle to high latitudes (see Figure 1). In the spring, column ozone reaches a peak in the middle to high latitudes due to the poleward transport of ozone-rich air from lower latitudes and higher altitudes [*Dobson et al.*, 1946; *Bojkov*, 1988]. In contrast, column ozone abundances in the autumn hemisphere are at least 30% smaller than the springtime maximum. Because large-scale planetary wave activity is at a minimum during the summer months, the decrease in total ozone has been largely attributed to in situ photochemical loss processes [*Johnston*, 1975; *Farman et al.*, 1985]. However, current models in general overpredict the decline of ozone through the summer months [*Chipperfield*, 1999]. This suggests that there is a need to better quantify the processes responsible for the decline in summertime ozone [*Natarajan and Callis*, 1997; *Rosenlof*, 1999].

The main objective for the Photochemistry of Ozone Loss in the Arctic Region in Summer (POLARIS) aircraft mission, completed in 1997, was focused on improving our understanding of the processes responsible for the decline in high-latitude ozone observed between Northern Hemisphere (NH) spring and autumn [*Newman et al.*, 1999]. The natural variability of stratospheric ozone must be well understood before accurate assessments of anthropogenic processes can be made. Therefore it was recognized that a concerted effort must be made to study and assess the accuracy of the ozone budget in this region of the atmosphere. The focus of this paper will be to further examine transport variations in the summer NH stratosphere and assess how well we can constrain the budget terms using available tracer and circulation fields.

The summer hemisphere has generally been characterized as a region of weak meridional circulation [*Brasseur and Solomon*, 1986; *Luo et al.*, 1997]. Because topographically forced large-scale planetary waves cannot propagate through the prevailing easterly winds present in the summer hemisphere [*Charney and Drazin*, 1961], eddy wave activity is relatively weak. Statistics from the National Centers for Environmental Prediction (NCEP) analysis show that amplitudes of wave 1-3 geopotential height are significantly weaker from June through September in the NH midlatitudes [*Randel*, 1987]. Previous observations of tracer variability in the summer stratosphere have been explained as either remnants of the springtime final warming or normal mode wave oscillations [*Ehhalt et al.*, 1983; *Hess and Holton*, 1985].

The variations in ozone and other trace gases in the summer stratosphere have been studied using various approaches. Results from a two-dimensional (2-D) model indicate that poleward of 40°N from 15 to 30 km, the net ozone loss during summer is due to photochemical destruction. This is attributed to the increased effectiveness of the odd nitrogen catalytic cycle [*Perliski et al.*, 1989; *Gao et al.*, 1999]. At lower latitudes, production and destruction are balanced by transport, while at higher altitudes, ozone is in photochemical equilibrium. However, the recent analysis of *Rosenlof* [1999] suggests that the seasonal cycle in transport is an important contributor to the summertime ozone budget between 60° and 70°N in the lower stratosphere.

Paper number 2001JD900004.
0148-0227/01/2001JD900004$09.00

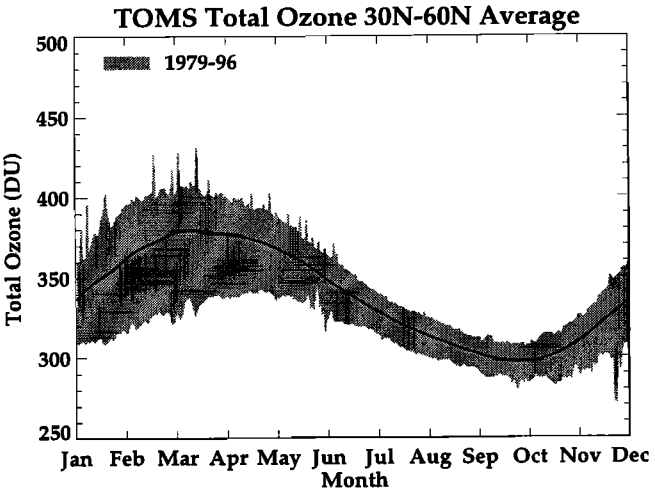

Figure 1. Time series of northern midlatitude total ozone between 30°N and 60°N averaged from 1987 through 1997. The thick line represents the time mean, while shading represents the range of values obtained from 1979 to1996.

Therefore understanding the impact of the transport circulation on tracer variability throughout the summer stratosphere is important for estimating the budgets of ozone and other tracers.

Estimates of the magnitude and direction of the transport circulation in the summer stratosphere from different analyses are varied. For example, diabatic heating rates computed from NCEP and the United Kingdom Meteorological Office (UKMO) analysis temperatures during July generally show atmospheric cooling poleward of 50°N below about 20 km, and atmospheric heating poleward of 60°N between 25 and 30 km in altitude. The altitude and latitude of the boundaries between heating and cooling, however, differ between the two analyses, with the region of discrepancy near 60°N. Heating (cooling) in the lower stratosphere implies rising (sinking) air motion and upward (downward) transport of lower (higher) ozone air to the region. *Eluszkiewicz et al.* [1997] compared heating rates using observations of temperature and radiatively active constituents from the Upper Atmosphere Research Satellite (UARS) Cryogenic Limb Array Etalon Spectrometer (CLAES) and Microwave Limb Sounder (MLS) instruments during 1992. Again, although the heating rates computed from the CLAES and MLS are generally similar, there are regions of disagreement including the summer NH. In this region the maximum difference in heating rates between the CLAES and MLS calculations is 0.1 K/d, compared to total heating rates of 0.5 K/d or less. This implies that calculated residual circulation fields in the summer stratosphere may have large uncertainties. A recent study investigating the utility of using global analyses for long-term transport studies finds that although mean winds and temperatures are broadly consistent with observations and other analyses, the accuracy of the residual circulation and the balance between residual circulation and wave transport remains uncertain [*Coy and Swinbank*, 1997]. The difficulty in obtaining accurate residual circulation fields remains a significant problem for long-term transport studies, and will be discussed further in this paper.

In this study we use a UARS climatology of long-lived tracer data along with estimates of the residual circulation to study the transport circulation of the NH summer stratosphere. This work is aimed at providing additional understanding of the dynamical contribution to the summertime decline of total ozone in the middle latitudes. Because CH_4 and HF are relatively long lived in the lower stratosphere, their variations can be used to understand transport processes. Estimates of the ozone budget are also made, including an attempt to derive the chemical rate. In section 2 we provide a brief description of the observational fields, while details of the summer variations of CH_4 and HF are shown in section 3. The calculation and description of the residual circulation are presented in section 4. In section 5 we use estimates of the transport fields to calculate the contributions of chemistry and dynamics on the HF and CH_4 budget during the NH summer stratosphere, while in section 6 we do the same for the ozone budget. The conclusions are given in section 7.

2. Observational Data

In this study we use a monthly climatology of Halogen Occultation Experiment (HALOE) Version 18 O_3, CH_4 and HF data between 100 hPa and 1 hPa during the years 1991-1997 as originally described by *Randel et al.* [1998]. Seasonal cycle fits to the monthly data are then made using a harmonic regression analysis. In the polar regions, where HALOE observations are absent, these analyses are augmented using CLAES CH_4 [*Roche et al.*, 1996] and MLS O_3 [*Froidevaux et al.*, 1996] observations, thus providing nearly global coverage. The UARS instrument HALOE uses a solar occultation sounding technique in the infrared to obtain vertical profiles of a number of atmospheric constituents [*Russell et al.*, 1993]. These measurements are obtained during daily sunrises and sunsets in the stratosphere and mesosphere. It takes about a month to obtain near-global coverage. The data have been mapped using potential vorticity from UKMO stratospheric analysis to more accurately represent vortex variations [e.g., *Lary et al.*, 1995]. A linear trend, determined over the period January 1993 through December 1996, has also been removed. More details of this climatology (hereafter referred to as the UARS climatology) can be found in the work by *Randel et al.* [1998] or on the HALOE web page (http://haloedata.larc.nasa.gov/home.html).

In the stratosphere, HALOE measurements of O_3, CH_4 and HF have varying degrees of accuracy. Data retrieval errors vary with altitude and, in general, increase in the lower stratosphere. Because we are using six years of HALOE observations, it is reasonable to assume that much of the random noise will be filtered out. Using the published systematic error estimates for O_3, CH_4 and HF [*Brühl et al.*, 1996; *Park et al.*, 1996; *Russell et al.*, 1996], we assume an accuracy of 10%, although we note that below 50 hPa, the error will likely be larger.

3. Tracer Distributions

In Figure 2 the climatological zonal mean distributions of CH_4, HF and O_3 during July are displayed. The contours of constant CH_4 and HF concentrations slope downward with increasing latitude, a reflection of the large-scale circulation which is characterized by upward motion in the tropics and descent over the higher latitudes. Atmospheric CH_4, which is produced at the Earth's surface, is destroyed in the stratosphere, and thus decreases with altitude in the stratosphere. Because tropospheric air predominately enters the stratosphere through the tropical stratosphere and is later transported to higher altitudes and latitudes, CH_4 concentrations generally decrease with increasing altitude and latitude due to photochemical processes. The opposite situation is observed with HF. Atmospheric HF has

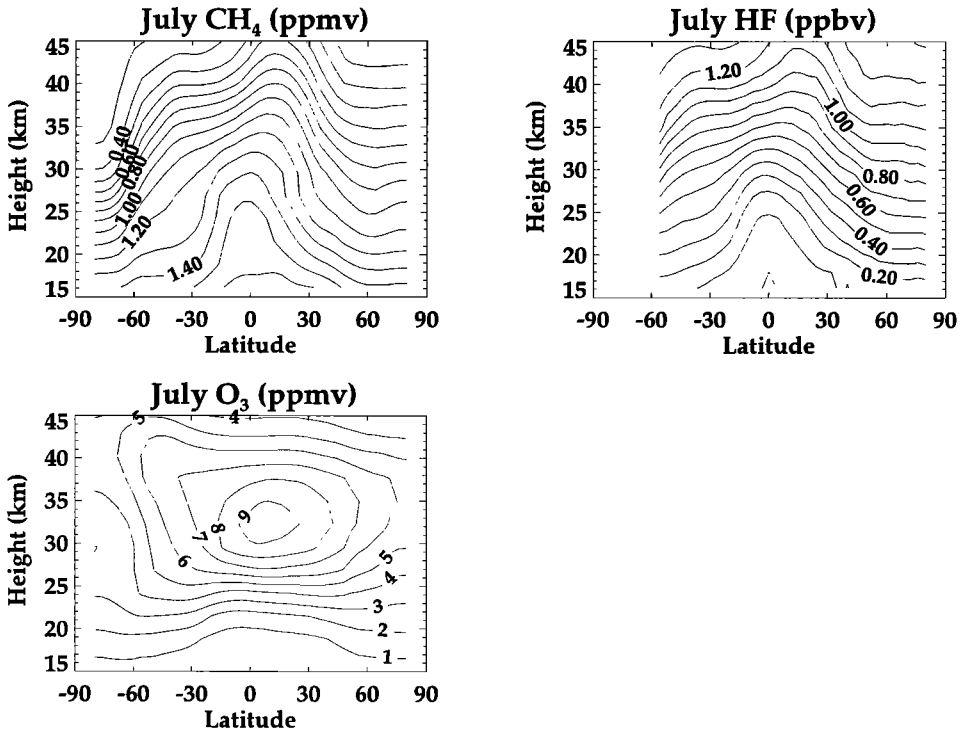

Figure 2. July distribution of CH_4, HF and O_3 obtained from the UARS climatology. The contour interval is 0.1 ppmv for the CH_4 distribution, 1 ppmv for O_3, and 0.1 ppbv for the HF.

no natural source in the troposphere; rather, HF is a by-product of CFC photolysis, which increases with altitude in the stratosphere. Thus stratospheric HF increases with altitude and, in general, increases with latitude. The distribution of O_3, shown in Figure 2, reaches a peak in the tropical latitudes near 34 km, reflecting the balance between production and loss processes, and decreases with latitude above about 20 km. Below 20 km, O_3 increases with latitude, ranging from 1 ppmv at 30°N to 2 ppmv at 70°N.

Variations in long-lived tracer concentrations can serve as indicators of transport processes and provide a means for understanding the dominant scales of motion present. Because HF and CH_4 are both relatively long lived in the lower stratosphere with lifetimes greater than several years, their seasonal variations can be linked to dynamical processes. We examine these dynamical variations and the consistency between the CH_4 and HF observations in the following manner. For analysis purposes we can assume that dynamical variations for long-lived tracers can be expressed as

$$\Delta\overline{\chi}_{\mathrm{dyn}} = \Delta\overline{\chi}_{\mathrm{obs}} - \int_0^{t_0} (P - L\overline{\chi}_{\mathrm{obs}})dt \qquad (1)$$

where $\overline{\chi}$ is the zonally averaged constituent field and $\Delta\overline{\chi}_{\mathrm{obs}}$ represents the observed constituent variation from time 0 to t_0. The chemical production (P) and chemical loss rates (L) for $\overline{\chi}$, in units of mixing ratio per second and per second respectively, are obtained from the NASA Goddard 2-D photochemical model [*Jackman et al.*, 1996]. Linear trends in CH_4 and HF are relatively small in the lower stratosphere compared to the seasonal variability and have been removed [*Randel et al.*, 1998]. Therefore using (1), we can estimate the change in the tracer field due solely to dynamics, $\Delta\overline{\chi}_{\mathrm{dyn}}$ over the timescale of a few months. In Figure 3 we show the percent change in CH_4 and HF concentrations due to dynamical variations, calculated from (1), at 32°N and 60°N during 2-month periods in early and late summer. Also displayed in the same plots are the total observed constituent tendencies, without the chemical terms removed. Although the chemical terms have little effect on CH_4 and HF concentrations in the lower stratosphere, with increasing altitudes chemistry becomes a significant fraction of the variability.

At 32°N, CH_4 concentrations due to dynamics increase from May through June between 15 and 33 km, while there is little change above 35 km. For the same time period, HF generally has the opposite tendency; decreasing concentrations below 33 km and small changes above 35 km. In general, anticorrelated variations in the CH_4 and HF fields are expected because of the oppositely oriented vertical and horizontal gradients of CH_4 and HF. From July through August, CH_4 and HF variations due to dynamics generally have larger amplitudes compared to early summer. HF changes are negative throughout the stratosphere, while CH_4 variations are small in the lower stratosphere and gradually increase with altitude. At 40 km, CH_4 concentrations increase by over 10% for the 2-month period, while HF concentrations decrease by 10% for the same 2-month period. Therefore while tracer changes in the lower stratosphere are similar between early and late summer, tracer tendencies at upper levels are much larger in July-August compared to the May-June period (Figure 3).

At higher latitudes the amplitudes of the changes in CH_4 and HF are smaller throughout the stratosphere and, in general, do not follow the pattern observed at 32°N. For the May-June period, although the anticorrelated behavior between variations in CH_4 and HF is observed, the magnitude of the variations does not differ significantly from zero considering the accuracy of the observations. Either transport processes are not as vigorous

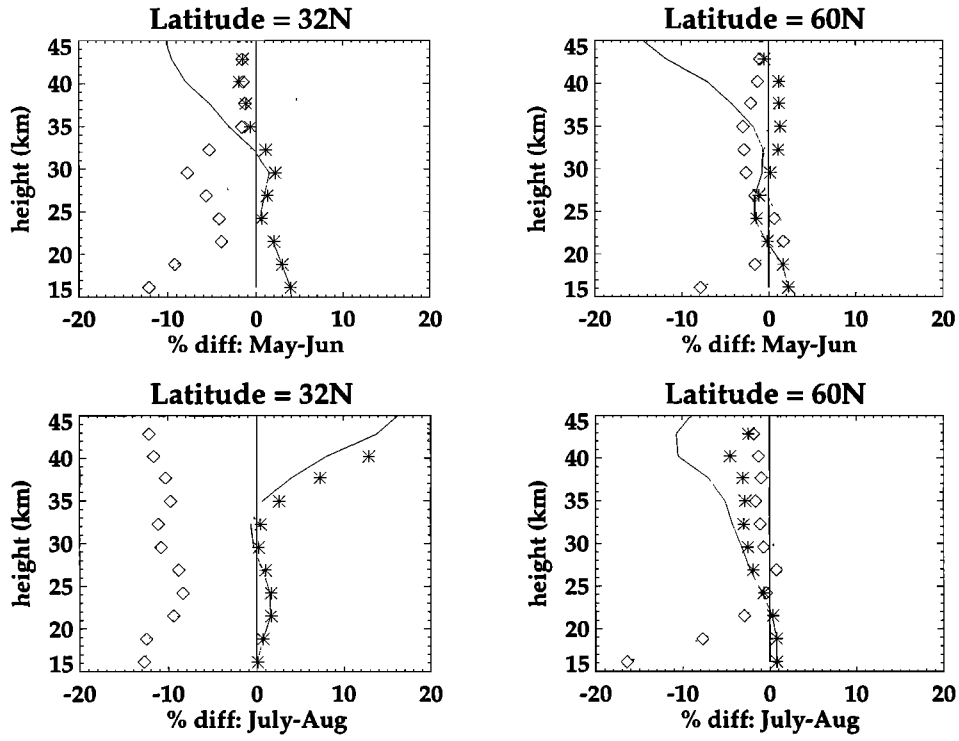

Figure 3. Percent difference change in UARS CH_4 and HF between May-June (top plots) and July-August (bottom plots) at 32°N (left plots) and 60°N (right plots). The star symbols indicate CH_4 variations while the diamond symbols represent HF variations. Tracer variations are given in percent difference, which is calculated as $100(\chi_{dyn}(\text{June}) - \chi_{dyn}(\text{May}))/\chi_{dyn}(\text{May})$, where χ_{dyn} is the zonal mean CH_4 or HF concentration with the chemical tendencies removed. The overlying solid and dashed lines represent the same percent difference calculation for CH_4 and HF, respectively, except that the chemical tendencies have not been removed.

during the high-latitude summer, or the horizontal and vertical processes partially cancel each other out. To better understand the magnitude and origin of these tracer variations and their implications for the ozone budget, we will now examine more closely the circulation of the NH summer stratosphere.

4. Residual Circulation

The residual circulation is estimated using the thermodynamic energy equation and mass continuity equations given as [*Rosenlof*, 1995]

$$\frac{\partial\bar{\theta}}{\partial t}+\frac{\bar{v}^*}{\cos\phi}\frac{\partial\bar{\theta}}{\partial y}+\bar{w}^*\frac{\partial\bar{\theta}}{\partial z}=\bar{Q} \tag{2}$$

$$\frac{1}{\cos\phi}\frac{\partial}{\partial y}(\bar{v}^*\cos\phi)+\frac{1}{\rho_0}\frac{\partial}{\partial z}(\rho_0\bar{w}^*)=0 \tag{3}$$

where $\bar{Q}$ is the zonal mean diabatic heating rate, $\bar{v}^*$ and $\bar{w}^*$ are the transformed Eulerian mean (TEM) residual circulation velocities and $\bar{\theta}$ is the potential temperature. The heating rates are calculated as described by *Rosenfield et al.* [1994], except that "effective" tropospheric cloud heights and amounts are included as in the work by *Rosenfield et al.* [1997]. In the thermodynamic energy equation, we have neglected the flux divergence terms, which are relatively small under quasi-geostrophic scaling [*Rosenfield et al.*, 1987]. Once the diabatic heating rates are calculated, the residual circulation can be calculated using an iterative method as originally outlined by *Murgatroyd and Singleton* [1961]. All calculations are based on data from the UARS-UKMO stratosphere-troposphere assimilation system [*Swinbank and O'Neill*, 1994].

Inherent in this procedure are uncertainties in the residual circulation calculation [*Shine*, 1989]. As discussed by *Eluszkiewicz et al.* [1997], qualitative differences in heating rates are found when different ozone and aerosol concentrations are used. In addition, the iterative procedure requires that the net vertical mass flux across a pressure level be zero when integrated across the latitudes. Thus we adjust $\partial\bar{w}^*/\partial z$ uniformly at all latitudes to satisfy the boundary conditions of $\bar{w}^*=0$ at the poles. Although uncertainties exist, *Rosenlof* [1995] found that the methods of calculating the residual circulation and the specific analyses used (e.g., UKMO or NCEP) did not produce significantly different circulation fields throughout the stratosphere. *Gettelman et al.* [1997] estimated that uncertainties of about 30% in the calculated vertical velocity at 50 hPa are present, while uncertainties are greater at lower altitudes. To help minimize the influence of year-to-year variations, and to be consistent with the UARS tracer climatology, we use heating rates averaged between 1993 and 1997. In the summer stratosphere, year to year variations in heating rates produce variation in the calculated residual circulation. For example, in the summer between 30°N and 60°N, interannual variations in $\bar{w}^*$ between 1993-1997 range from 0.1 to 0.2 mm/s or about 30% of the mean. The implication of these variations on tracer budget calculations will be discussed further in section 5.

In Figure 4 we show global $\bar{w}^*$ fields averaged over May-June and July-August. During both periods the large-scale

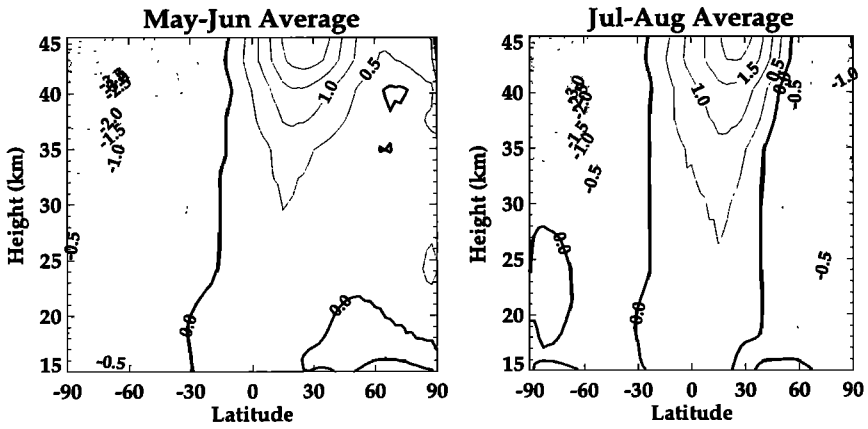

Figure 4. Global $\overline{w}^*$ fields averaged from 1993 through 1997 and for May-June and July-August. Units are in millimeters per second, where the dashed contours denote downward motion and the thick line denotes the zero contour.

circulation pattern shows weak upward motion in the tropical latitudes and strong downward motion in the winter polar latitudes. The down-welling in the high latitude winter hemisphere is strong, reaching a magnitude of 8 mm/s in July at 45 km. In the tropics, $\overline{w}^*$ ranges from 0 to 1 mm/s in the lower stratosphere, and up to 2 mm/s in the upper stratosphere near 45 km. These values are very similar to other estimates of the residual circulation [*Rosenfield et al.*, 1987; *Eluszkiewicz et al.*, 1997].

In the NH stratosphere there is a distinct change in the circulation from early summer (May-June) to late summer (July-August). In the early summer, upward motion is found throughout most of the NH stratosphere, except for an area in the lower midlatitude stratosphere between 15 and 20 km in altitude. In this region, weak downward motion (-0.1 to -0.3 mm/s) is a persistent feature in both the climatological mean and every individual year between 1993 and 1997. Throughout the rest of the NH early summer stratosphere, weak upward motions ranging from 0.1 mm/s to 0.5 mm/s are observed. In middle to late summer, the circulation changes to predominately downward motion poleward of 40°N. Down-welling becomes increasingly stronger in the NH through September and October, as the atmospheric circulation transitions through the equinox toward the winter season. During July-August, downward velocities

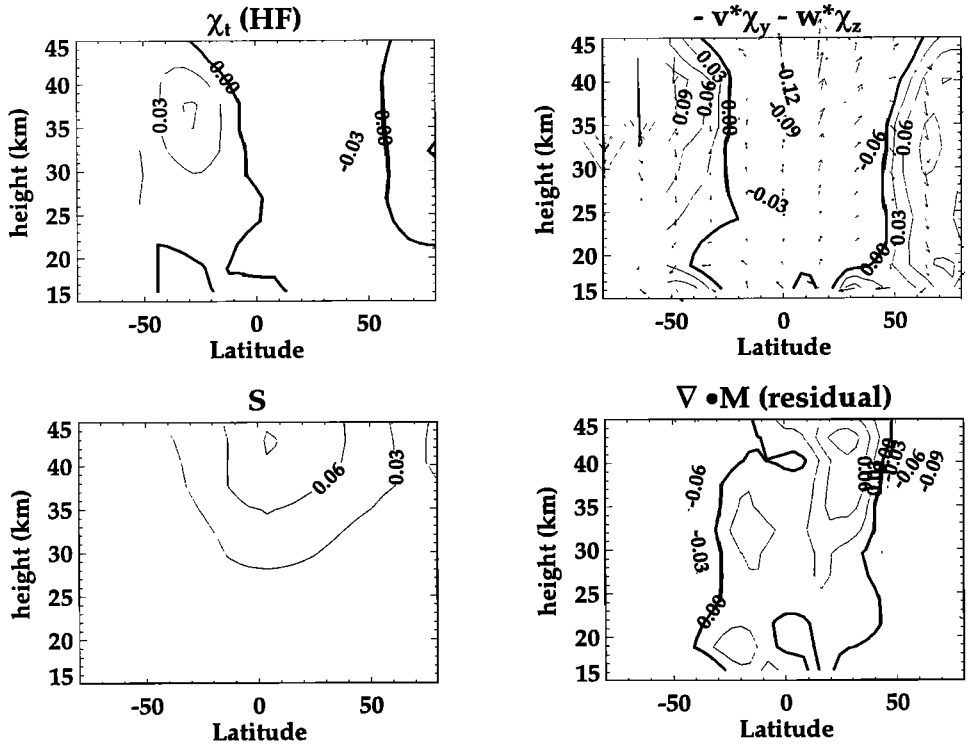

Figure 5. Meridional cross section of individual terms in HF budget (equation (4)) for May-June period. Contour interval is 0.03 ppmv/month, where dashed contours denote negative tendencies and the thick line denotes the zero contour. Vectors in upper right cross section denote the components of the residual circulation. See text for more details.

range from -0.2 mm/s to -0.6 mm/s in the lower stratosphere, to near -1 mm/s in the upper stratosphere. In the record from 1993 through 1997, the transition from predominately upward motion in the early summer to downward motion in the middle to late summer normally occurs in July. The calculations of *Eluszkiewicz et al.* [1997] show a similar transition during 1992. An examination of how this transition in transport influences HF and CH_4 budgets will be discussed in the next section. This information will be later used to study the role of transport in the ozone budget in the summer stratosphere.

5. Budget Calculations: HF and CH_4

The tracer continuity equation in the meridional plane can be written as [*Andrews et al.*, 1987]

$$\frac{\partial \overline{\chi}}{\partial t} + \frac{\overline{v}^*}{\cos\phi}\frac{\partial \overline{\chi}}{\partial y} + \overline{w}^*\frac{\partial \overline{\chi}}{\partial z} = \overline{S} + \nabla \bullet \mathbf{M}. \quad (4)$$

The eddy transport term, which represents the flux divergence due to wave disturbances, can be approximated as [*Sabutis*, 1997]

$$\nabla \bullet \mathbf{M} = \frac{1}{(\cos\phi)}\frac{\partial}{\partial y}\left(\cos\phi K_{yy}\frac{\partial \chi}{\partial y}\right), \quad (5)$$

where the term K_{yy} is the horizontal diffusion coefficient. In the stratosphere the influence of vertical diffusion (modeled as K_{zz}) is assumed to be small [*Sabutis*, 1997] and will be neglected in this study.

We can now quantify the relative contributions of the various terms in the constituent continuity equation (4). The tracer gradients, both in space and time, are calculated from the UARS climatology using finite differences to approximate the gradients. The chemical term, S, is obtained from the NASA Goddard 2-D model, while the residual circulation is calculated as explained in section 4. The remaining unknown is the eddy transport. Because this term is inherently difficult to calculate explicitly, for now we estimate the contribution due to eddy transport as a residual of the other terms in (4). We will later explore other methods for estimating the eddy transport.

5.1. HF

Figure 5 shows the structure of the individual components for the HF budget averaged for the May-June period. The data gaps are because the HALOE observing pattern does not sample latitudes poleward of 60°S during the NH summer. In the tropical latitudes the time tendency term, $\overline{\chi}_t$, is positive, indicating an increase in local concentration. At higher northern latitudes, negative tendencies are present below 30 km in altitude. The mean meridional transport, $-\overline{v}^*\overline{\chi}_y - \overline{w}^*\overline{\chi}_z$, produces the largest HF tendencies in the upper stratosphere. At 40 km in altitude, large negative tendencies are found in the northern subtropics, while large positive tendencies occur in the southern middle latitudes. Inspection of the residual circulation vectors (denoted by the arrows) suggests that $\overline{w}^*\overline{\chi}_z$ is the more important component for the mean transport. The chemical terms are significant only in the upper stratosphere, reflecting the photodissociation of CFCs and their conversion to HF. The eddy transport, $\nabla \bullet \mathbf{M}$, calculated as a residual, has a hemispheric structure similar to the mean meridional transport, but with the opposite sign. Although the calculation of $\nabla \bullet \mathbf{M}$ also includes any errors associated with this analysis, the structure is generally similar to other estimates of the horizontal diffusion [*Randel et al.*, 1998].

In Figure 6 the HF budget terms are shown for the July-August period. There is a larger area of negative HF tendencies in the NH for the July-August months compared to the May-June period. For $-\overline{v}^*\overline{\chi}_y - \overline{w}^*\overline{\chi}_z$, there are strong tendencies in the tropical upper stratosphere and in the high latitudes. In particular, poleward of 50°N the downward circulation produces

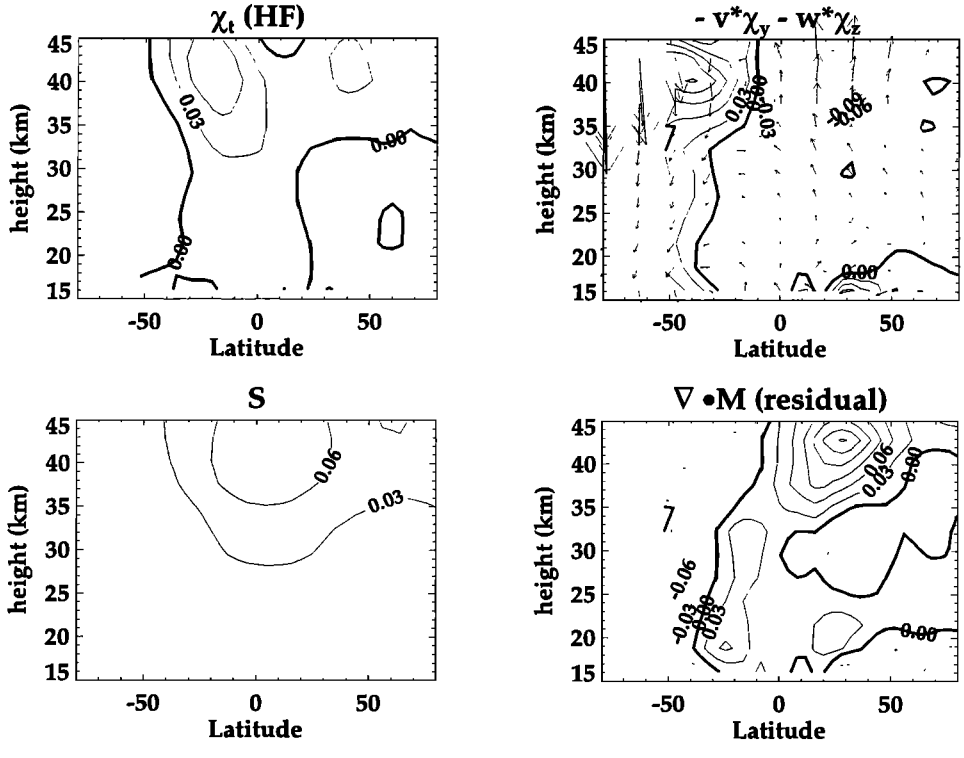

Figure 6. As in Figure 5, except for the July-August period.

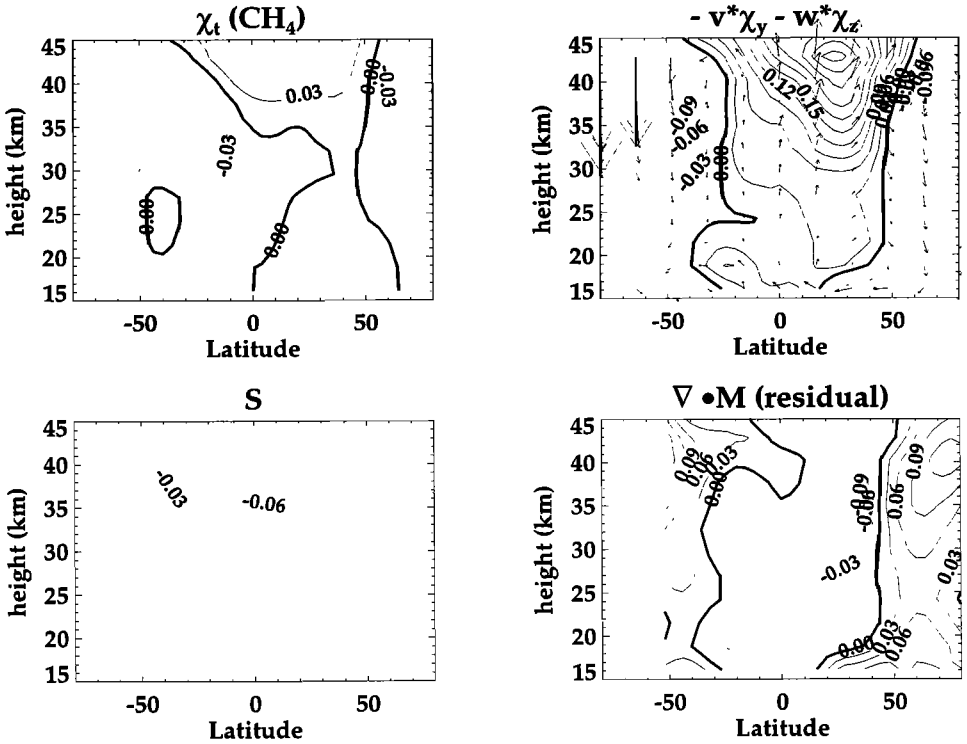

Figure 7. As in Figure 6, except for CH_4.

HF tendencies up to 0.1 ppbv/month. Correspondingly, $\nabla \bullet \mathbf{M}$ is also larger in July-August. Again, the structure and distribution are similar to the mean meridional transport, with negative tendencies calculated poleward of 50°N. The relative balance between the mean meridional transport and the eddy transport are an apparent feature of the stratosphere [*Randel et al.*, 1998].

In the NH at middle to high latitudes, there are significant differences in transport tendencies between early and late summer. In the early summer, when the time tendency is mostly negative poleward of 30°N, the presence of weak upward motion can largely explain these tendencies. In addition, the magnitudes of the mean meridional transport and the eddy transport are similar to the time tendency. After June, this situation changes significantly. From July through August, the magnitudes of $-\overline{v}^* \overline{\chi}_y - \overline{w}^* \overline{\chi}_z$ and $\nabla \bullet \mathbf{M}$ are 2 to 3 times as large as the time tendency, $\overline{\chi}_t$. Thus the balance in the HF budget in the high-latitude stratosphere becomes a difference of two larger competing terms, while the time tendency and chemical terms are significantly smaller.

Uncertainties in these calculations must also be considered. The uncertainties in the tracer climatology, as discussed in section 2, are assumed to be at the 10% level. We assume that tracer gradients have similar uncertainties. The calculation of the residual circulation may also have large uncertainties as discussed in section 4 and in the work by *Gettelman et al.* [1997]. Using the standard deviation of the residual circulation, calculated from different years, gives an estimate of the variability in these fields. This suggests that transport tendencies due to the residual circulation may have an uncertainty of 40% or larger in the summer NH stratosphere. If we assume that the chemical rates are known within 10%, then estimates of the eddy transport, calculated as a residual, may have uncertainties of 50% or more. We note that these uncertainties are particularly large, in part, because of the weak transport circulation present in the summer stratosphere. Similar calculations in the winter latitudes are likely to have a lower uncertainty because of the larger heating rates [*Gettelman et al.*, 1997].

5.2. CH_4

Because CH_4 and HF have similar spatial gradients, we expect the structure of the budget calculations to be similar, but of opposite sign. In general, we find this to be true. Figure 7 shows the structure of the individual CH_4 budget terms during the July-August period. In comparison with Figure 6, the structure of $-\overline{v}^* \overline{\chi}_y - \overline{w}^* \overline{\chi}_z$ is very similar to the corresponding HF term, except with the opposite sign. The upward motion of the tropical latitudes produces positive tendencies in CH_4, while the downwelling of the NH higher latitudes produces negative tendencies. The boundaries between the positive and negative tendencies in the CH_4 and HF budgets are closely collocated, in addition to the locations of the relative minimum and maximum values. Again, this is not surprising considering the similarity between the spatial gradients of CH_4 and HF (see Figure 2). There are also strong similarities between the CH_4 and HF structures for $\nabla \bullet \mathbf{M}$, although small differences exist as well. The origin of the differences largely resides in the chemical and time tendency terms, which are both slightly different between CH_4 and HF. The good correspondence between the CH_4 and HF data sets is an indication of the relative consistency between the UARS observations [*Park and Russell*, 1994]. In the next section, we will use the good correspondence between these datasets to derive additional estimates of the eddy transport.

5.3. Estimates of Eddy Transport

In the above analysis, although we have identified the general tendencies of the tracer budgets, an independent method of calculating the eddy transport would be desirable. If accurate

estimates of the eddy transport could be obtained, then the tracer observations, along with the residual circulation calculations, could be used to constrain the chemical terms as a residual. While the eddy transport can be calculated directly from observations, in practice this is quite difficult, and thus simplifying assumptions are generally made to allow the use of global analyses to calculate the eddy diffusion coefficient [*Newman et al.*, 1988]. Estimates of the horizontal eddy diffusion coefficient, K_{yy}, can be calculated using the UKMO global analyses as described by *Jackman et al.* [1996]. Briefly, the Eliassen-Palm (E-P) flux divergence is computed off-line from the UKMO 3-D analyses from 1990 through 1997. The horizontal diffusion coefficient is then obtained by computing the ratio of E-P flux divergence to the meridional gradient of zonal mean potential vorticity [*Randel and Garcia*, 1994]. We will neglect the influence of the vertical diffusion, K_{zz}, which is relatively small in the stratosphere [*Sabutis*, 1997].

Calculations of the HF eddy transport using (5), where K_{yy} is estimated from the UKMO analyses, are compared to the residual calculations. Although the sign of the tendencies is generally consistent between the two techniques, in general the magnitudes are weaker using the eddy diffusion coefficient, especially in late summer at high latitudes. Similar results are obtained using the CH_4 constituent data. There are two possible reasons for the poor correspondence between these two methods. First, because of the relatively weak large-scale wave motions present in the summer stratosphere, estimates of the eddy transport may not be as useful during this time of year. Second, since the calculations of (5) require computing a second derivative of the observed tracer fields, any inherent uncertainties in the initial tracer field will be amplified after two derivative operations. Therefore it is difficult to argue that improvements in our understanding of the magnitude of the eddy transport in summer have been made with this method.

We now consider an alternate method to derive the eddy diffusion coefficient using the previously derived tracer budgets. If we assume that the residual term is the complete horizontal eddy transport term, then from (5), we can solve for K_{yy} using the calculated residual. This calculation, however, produces extremely noisy fields, and thus the results are not usable. However, we find that using a simpler relationship between $\nabla\bullet\mathbf{M}$ and K_{yy} yields structures that reproduce most of the observed variations in the $\nabla\bullet\mathbf{M}$ term. We define an effective diffusion coefficient as $K'_{yy} = -a(\nabla\bullet\mathbf{M})/(\tan\phi\bar{\chi}_y)$, where a is the Earth's radius. Note that this is simply one of the terms in the expanded derivative of (5); the other two terms are generally smaller in magnitude [*Holton and Choi*, 1988]. Calculations of the eddy transport using the effective diffusion coefficient can then be made.

In Figure 8, we show the HF eddy transport calculated using the effective diffusion coefficient derived from the CH_4 calculations. Overall, the eddy transport calculation using the effective diffusion coefficient is very similar to the residual calculation of $\nabla\bullet\mathbf{M}$, shown in Figures 5 and 6. This is again expected because of the similarity in the transport tendencies between HF and CH_4 observations. The large-scale features of the residual calculation are well captured in the effective transport calculation, although at high latitudes during July-August, the effective transport calculation is somewhat weaker. In section 6, we will use these effective transport coefficients to estimate the magnitude of eddy transport for the summertime ozone budget.

6. Ozone Budget Analysis

6.1. Total Ozone Observations

As described in section 1, the total ozone field in the NH decreases by a sizeable portion from spring through the fall. For example, between 30°N and 60°N, average total ozone values reach a maximum of approximately 380 Dobson units (DU) during March and April, and fall to below 300 DU by October (see Figure 1). At higher latitudes the seasonal variation between spring and fall is even more pronounced; total ozone values at 75°N decrease by almost 40% from a maximum of 460 DU in spring to a minimum of 280 DU in the fall.

In Figures 9a and 9b, total ozone fields (hereafter referred to as UTOZ) for April and September are calculated from the UARS climatology and compared with zonal mean TOMS observations averaged between 1979 and 1997. Because the UTOZ calculations only represent ozone concentrations above 100 hPa, we expect the TOMS measurements to be larger in magnitude as they represent the entire column including the lower stratosphere and troposphere. Indeed, we find that UTOZ observations are between 65 and 80% of the TOMS values depending on the latitude and time of year. In April, TOMS total ozone increases sharply with increasing latitude in the NH, while significantly smaller changes are found with the UTOZ observations. This is especially true poleward of 45°N, where as the TOMS gradient sharpens, the UTOZ gradient remains relatively flat. Equatorward of 40°N, UTOZ is around 80% of

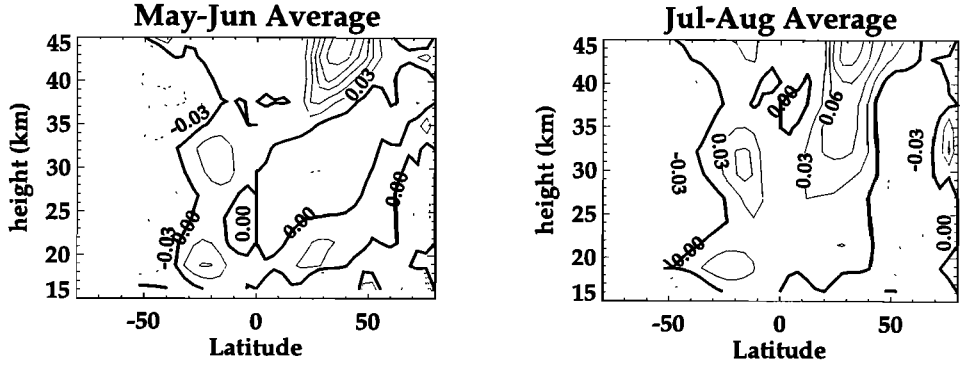

Figure 8. Transport tendency for HF due to horizontal eddy transport calculated using the effective transport diffusion coefficient for periods averaged in May-June and July-August. Contours are in 0.03 ppbv/month, where dashed contours denote negative tendencies and the thick line denotes the zero contour. See text for more details.

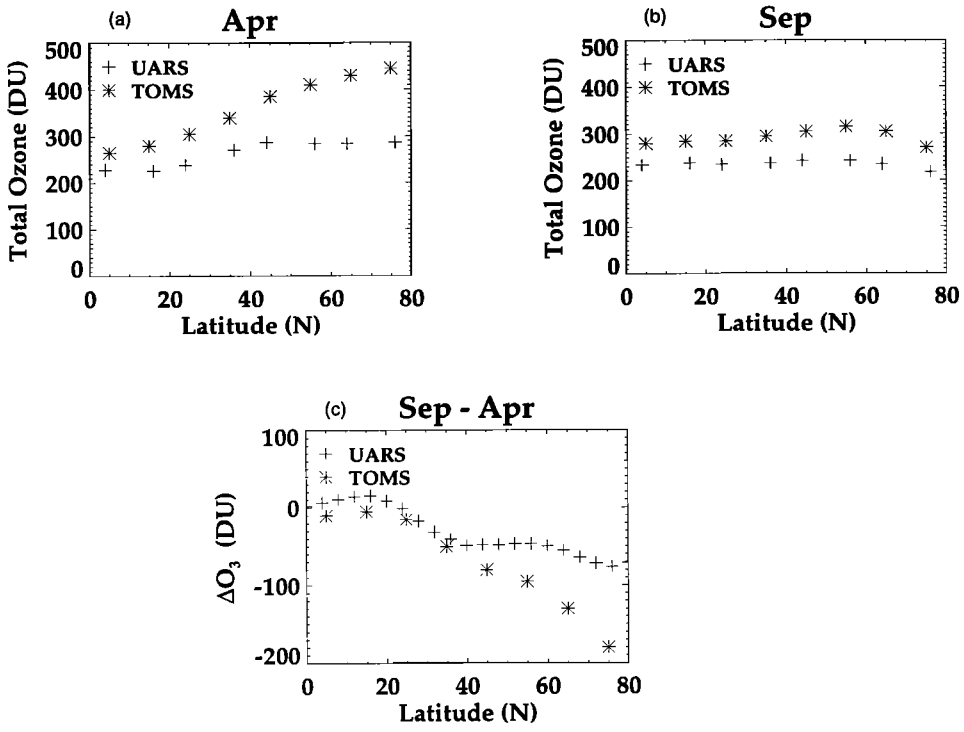

Figure 9. Average total ozone for (a) April and (b) September, and (c) change in total ozone between April and September, calculated from the UARS O_3 observations (pluses) and 1979-1993 TOMS observations (asterisks).

the TOMS measurements, while poleward of 50°N, the UTOZ is only 65% of the TOMS observations. In September, however, the difference between UTOZ and TOMS is constant with latitude; throughout the NH during September, UTOZ accounts for 75-80% of the column ozone observed by TOMS. An explanation for the changes between April and September can be found through examination of the ozone profiles. April ozone profiles at higher latitudes appear shifted downward in altitude by 2-3 km compared with profiles in September. Thus in April, more of the ozone column resides below 100 hPa than in September.

The amount of ozone lost during the summer months in the northern latitudes, calculated from both UARS and TOMS, is shown in Figure 9c. At lower latitudes, UTOZ and TOMS roughly agree. The declines in total ozone from April to September increase in magnitude with increasing latitude up to 40°N, where the total decline of ozone is nearly 60 DU through the summer. At higher latitudes, the decline in total ozone during summer increases sharply with latitude according to TOMS, while the change in UTOZ is roughly constant with latitude. For example, at 65°N the decline of ozone during summer from UTOZ is 60 DU compared to a decline of 140 DU from TOMS. The variations in these differences suggest that a significant proportion (35-55%) of the high-latitude summertime ozone decline poleward of 50°N occurs below 100 hPa, the lowest pressure level observed by HALOE. Therefore the following ozone budget analysis, which is only valid down to 100 hPa, may only represent a portion of the total ozone variability.

6.2. Ozone Budget

We now calculate the ozone budget terms in a manner similar to section 5 using the previously derived estimates of the transport circulation. In Figure 10 the structure of the individual ozone budget terms is shown, where the transport tendencies are only shown up to 30 km. Above 30 km, ozone is in photochemical equilibrium and thus responds much more rapidly to chemical variations than dynamical variations, while at 25 km the chemical and dynamical timescales are both near 100 days [*Brasseur and Solomon,* 1986]. Therefore although we show the analysis up to 30 km, we realize that from 25 to 30 km, changes in the local chemistry may play a larger role than transport.

The observed ozone tendency in early summer is negative in the NH lower stratosphere poleward of 20°N (Figure 10a). The transport due to the mean meridional circulation produces negative tendencies over much of the NH stratosphere, except for a region in the lower stratosphere poleward of 20°N. Chemically, there is production in the tropical latitudes and destruction in the higher latitudes, while the magnitudes of the chemical terms above 25 km are large compared to the dynamical terms. In the later summer (Figure 10b) the presence of strong downward motion poleward of 40°N produces larger transport amplitudes due to the mean meridional circulation. The positive tendencies are explained by downward motion bringing higher ozone air to lower altitudes. We note that the timing and distribution of the O_3 tendencies are similar to the HF results.

Table 1 shows the individual contributions to the ozone budget for the NH at 19 and 24 km for latitudes in early and late summer. In general, the observed ozone tendencies are larger in early summer compared to late summer. The chemical terms, obtained from the Goddard 2-D model, are also larger in the early summer months. However, the opposite tendency is found with the meridional and eddy transport at latitudes poleward of 55°N. In early summer the meridional transport tendencies are only half as large is the late summer tendencies. For example, at 55°N and 19 km in altitude, during early summer the contribution from the residual circulation is +0.14 ppmv/month, compared to +0.35

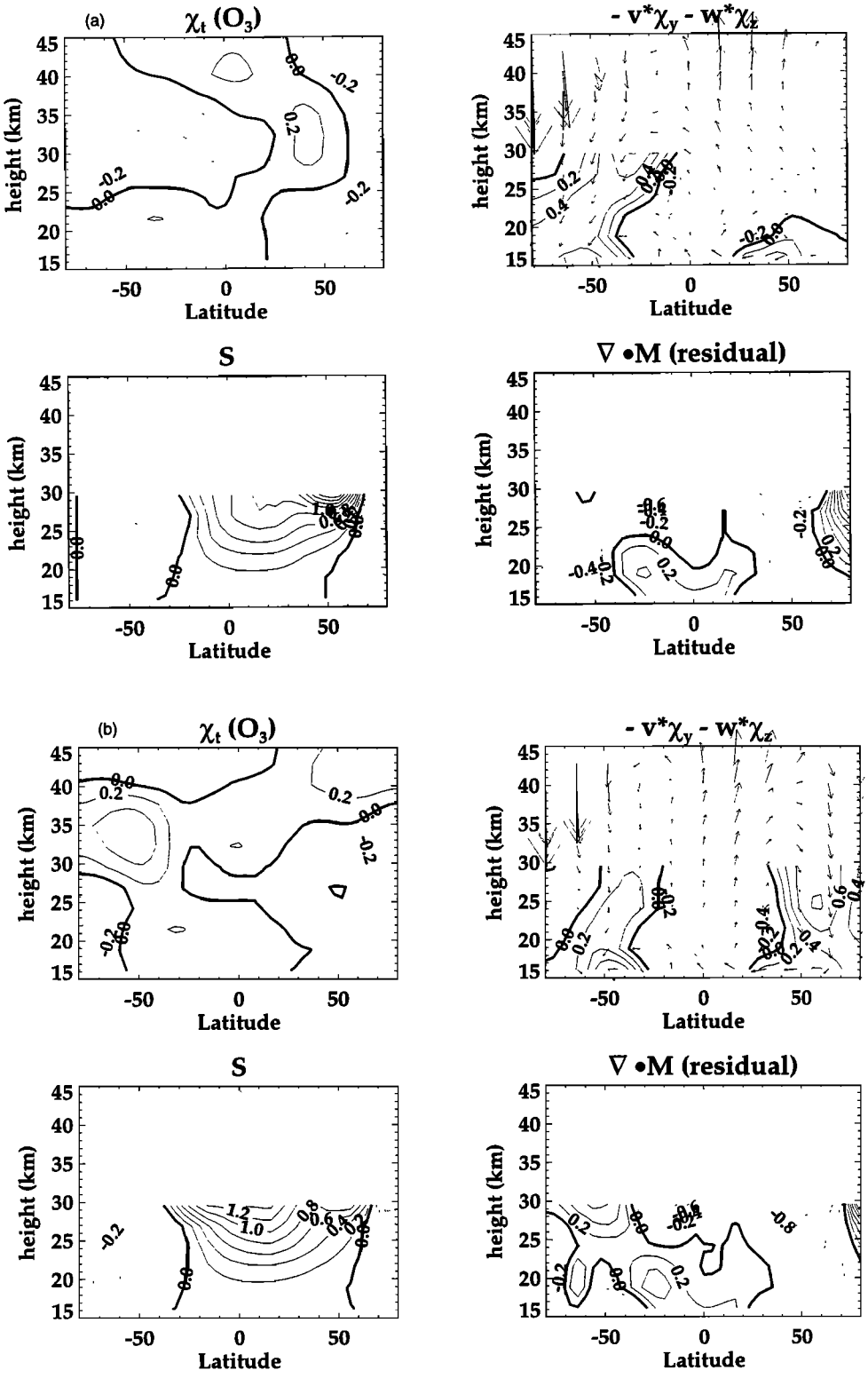

Figure 10. As in Figure 5 except for O_3 during (a) May-June and (b) July-August.

ppmv/month in late summer. This change is also found in the eddy transport term, which is calculated as a residual. As discussed earlier, the reason for these changes is largely due to the increased strength of the residual circulation in late summer. These results compare well with the zonally averaged ozone mass flux calculations of *Gettelman et al.* [1997] and *Rosenlof* [1999], which show the distinct change in transport tendencies between the early and late summer. These results suggest that chemistry is a larger proportion of the ozone budget in the early summer compared the later summer months.

The contribution of these variations to the total ozone is shown in Figure 11. The ozone tendencies, integrated between 100 and 31 hPa, are calculated from April through September. The time tendency of ozone shows a maximum decrease of 15 DU/month

Table 1. Ozone Tendencies for the Individual Terms Given in Equation (4)[a]

	May-June Average				July-August Average			
Latitude/Height	$\overline{\chi}_t$	$-(\overline{v}^*\overline{\chi}_y+\overline{w}^*\overline{\chi}_z)$	S	$\nabla\bullet\mathbf{M}$	$\overline{\chi}_t$	$-(\overline{v}^*\overline{\chi}_y+\overline{w}^*\overline{\chi}_z)$	S	$\nabla\bullet\mathbf{M}$
40°N 19 km	-0.24	-0.06	0.05	-0.24	-0.02	0.02	0.06	-0.10
55°N 19 km	-0.20	0.14	-0.04	-0.30	-0.07	0.35	-0.01	-0.42
70°N 19 km	-0.17	0.02	-0.14	-0.05	-0.03	0.49	-0.09	-0.43
40°N 24 km	-0 08	-0.24	0.44	-0.28	-0.05	0.08	0.39	-0.52
55°N 24 km	-0.14	-0.21	0.23	-0.16	-0.01	0.81	0.15	-0.97
70°N 24 km	-0.26	-0.29	-0.41	0.44	-0.13	0.49	-0.37	-0.26

[a]Units are in ppmv/month.

during May poleward of 35°N. The column ozone tendencies then decrease in amplitude until September, when the tendencies begin to increase though the NH middle latitudes. The tendencies due to the residual circulation, chemistry and the eddy transport are also shown in Figure 11. The contribution of dynamics (residual circulation and eddy mixing) is large compared to the chemistry and time tendency, as mentioned previously. In general, the mean meridional transport acts to increase the ozone column throughout the summer months poleward of 35°N, while the eddy transport acts to decrease the ozone column poleward of 25°N. Physically, this can be explained as the mean meridional circulation's transporting higher-ozone air to higher latitudes (positive tendency), while the quasi-horizontal eddy transport is bringing lower-ozone air from the tropics to higher latitudes (negative tendency). *Rosenlof* [1999] also found that the contribution of eddy transport to the ozone budget is largely negative in the lower stratosphere at 60°-70°N in the middle to late summer.

Uncertainties in these calculations are similar to those obtained for the HF fields; uncertainties in the residual circulation term and eddy transport term may be as large as 50% or more. The combined uncertainties in the observed time tendency and chemical terms are estimated to be between 10% and 20%.

6.3. Estimates of the Ozone Chemical Rate

In theory, it should be possible to use the previously derived budget terms to obtain estimates of the chemical rates as a residual. In section 5, estimates of the horizontal eddy diffusion coefficient from UKMO analyses were used to calculate the eddy transport. These fields, however, did not resemble the residual eddy transport term, and thus it does not seem that deriving a chemical rate in this manner would produce meaningful results. More encouraging results were produced using the effective diffusion coefficient, which did produce eddy transport fields that resembled the residual eddy transport calculation. Therefore we now attempt to derive the ozone chemical rate as a residual of the other budget terms.

Figure 12 shows the ozone chemical rate calculated as described above. These results indicate that between 16 and 24

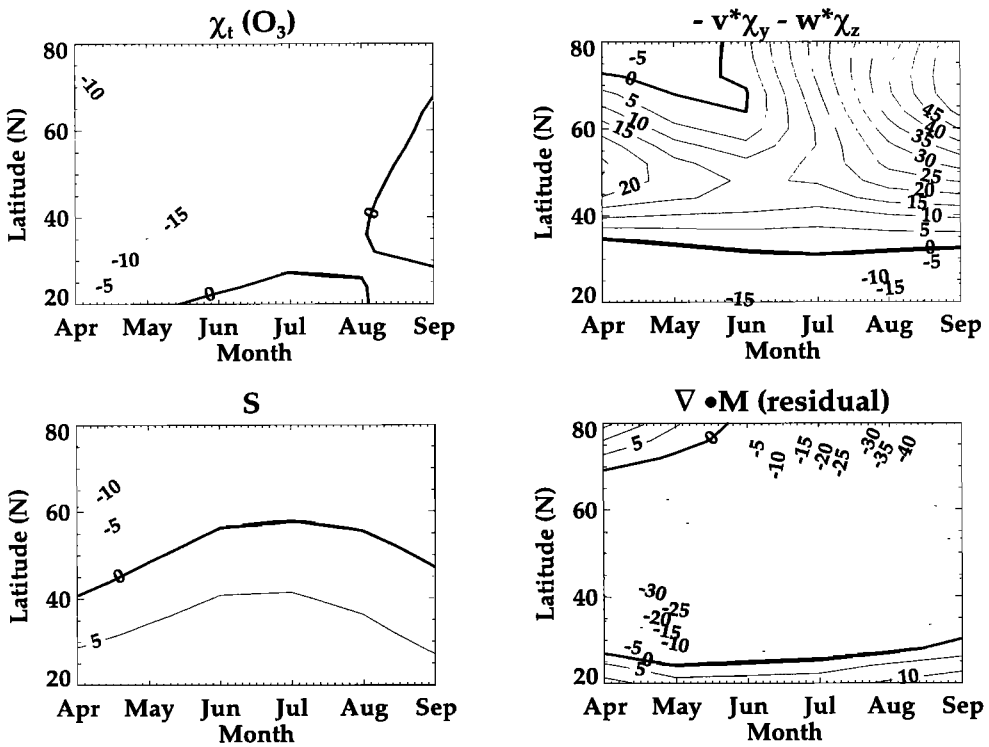

Figure 11. Time series of individual ozone tendencies integrated from 100 to 31 hPa for $\overline{\chi}_t$, $(-v^*\chi_y - w^*\chi_z)$, $\overline{S}$ and $\nabla\bullet\mathbf{M}$, calculated as a residual. Contour intervals are in 5 DU/month, where dashed contours denote negative tendencies and the thick line denotes the zero contour.

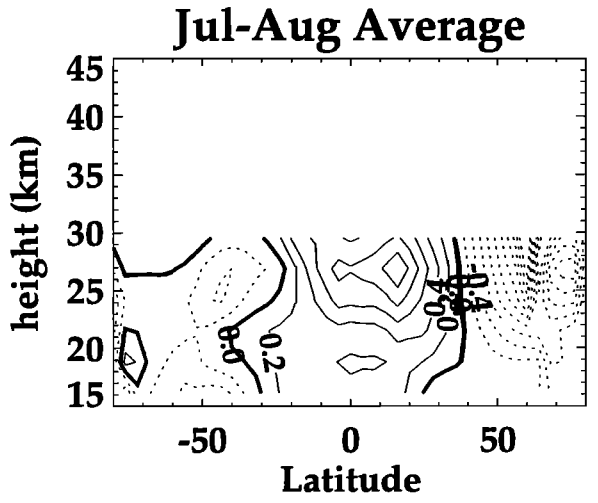

Figure 12. Chemical rate of ozone during July-August calculated as a residual from the other budget terms. Contour interval is in 0.2 ppmv/month, where dashed contours denote regions of chemical destruction, and the thick line denotes the zero contour.

km, chemical ozone production is present in the tropical latitudes extending to about 40°N, while chemical loss is present at the higher latitudes. While, in general, these results seem reasonable, the uncertainties in the calculations of these rates are significant. Even with our somewhat conservative estimates of the uncertainties in the tracer fields (section 2), residual circulation (section 4) and eddy transport derived from the CH_4 fields (section 5), the derived chemical terms have uncertainties of 110% or larger. Considering the large uncertainties in the derived ozone chemical rate, this method at present is not useful for constraining the chemical rates of the ozone budget in the summer NH stratosphere. Better estimates of the residual circulation and eddy transport in the summer stratosphere are required before more accurate and useful estimates of the ozone chemical rate can be inferred from observations such as these.

7. Conclusions

Tracer budget fields derived from HF and CH_4 are used to investigate dynamical variations in the summer Northern Hemisphere stratosphere. These results are then later used to study the role transport plays in the summertime ozone budget. A tracer climatology from UARS and estimates of the residual circulation derived from UKMO temperature analyses are used to determine transport tendencies. Estimates of the eddy transport are first determined as a residual of the other budget terms, and then later estimated from CH_4 tracer budgets. The structure and amplitude of the individual terms in the constituent budget equation were then analyzed.

There are significant changes in the transport circulation of the NH stratosphere from early summer (May-June) to late summer (July-August). In early summer, upward motion is present throughout much of the NH stratosphere, while in the later summer months, downward motion is prevalent poleward of 40°N. This has an important impact on long-lived tracer budgets. For HF, upward motion in early summer produces negative tendencies, while downward motion in late summer produces positive tendencies. In early summer, transport by the residual circulation can account for a majority of the tracer variability, while by middle to late summer, the mean meridional transport and eddy transport terms, which largely oppose each other, are much larger than the observed tracer tendency. The balance between these two larger terms in the middle to late summer (the chemical term is normally small for CH_4 and HF in the lower stratosphere) makes model calculations of tracer tendencies during middle to late summer challenging. This is especially true considering the relatively large uncertainties identified in calculations of the residual circulation and the eddy transport in the NH summer.

We perform a similar budget analysis for lower stratosphere ozone. UARS observations show that ozone loss occurs primarily in early summer, and in the lowest levels of the stratosphere. A comparison of UARS and TOMS total ozone suggests that 35%-55% of the summertime ozone loss occurs below 100 hPa poleward of 50°N. Ozone budget analyses show that chemical rates alone (from the Goddard 2-D model) are not sufficient to produce the declines in ozone observed through the summer months.

In early summer the relatively weak residual circulation produces positive ozone tendencies throughout much of summer stratosphere. The magnitudes of these tendencies, along with the tendencies of eddy transport and chemistry, are all similar to the observed ozone tendency. However, by late summer, the residual circulation becomes strongly downward in the higher latitudes. The contributions to the ozone budget by the residual circulation and eddy transport are now a factor of 2 to 3 times larger than the observed ozone tendency. This implies that in the late summer the balance between two relatively large transport terms and a chemical term produces the relatively small ozone decreases observed.

We also explored deriving the ozone chemical rate as a residual of the other budget terms. At present, though, the relatively large uncertainties in the individual transport terms do not provide enough accuracy to adequately constrain the ozone chemical rate. In particular, uncertainties in the residual circulation field and the eddy transport are estimated to be significant, although their magnitudes largely cancel each other in the summer stratosphere. While our analysis is in general agreement with previous studies, large uncertainties persist in our calculations of transport budgets in the summer stratosphere. The difficulty in calculating accurate transport fields in the summer stratosphere, as also noted by *Coy and Swinbank* [1997], is primarily due to the presence of relatively weak heating rates in the NH summer. Thus, obtaining accurate estimates of the relative balances between dynamics and chemistry is particularly difficult in the NH summer stratosphere and will require further work before useful constraints can be placed on the budget terms.

Acknowledgments. The authors would like to thank W. J. Randel for developing the very useful UARS climatology, E. Fleming for the Goddard 2-D model chemical rates and J. Rosenfield for the radiative heating calculations. We also thank L. Coy for his many helpful discussions. We would also like to acknowledge J. M. Russell III, A. E. Roche and J. W. Waters, the respective PIs of the HALOE, CLAES and MLS instruments. Partial support for E.C.C. was provided through the UARS Guest Investigator Program.

References

Andrews, D. G., J. R. Holton, and C. B. Leovy, *Middle Atmosphere Dynamics*, 498 pp., Academic, San Diego, Calif., 1987.

Bojkov, R. D., Ozone variations in the northern polar region, *Meteorol. Atmos. Phys.*, *38*, 117-130, 1988.

Bowman, K. P., and A. J. Krueger, A global climatology of total ozone from the Nimbus 7 Total Ozone Mapping Spectrometer, *J. Geophys. Res.*, *90*, 7967-7976, 1985.

Brasseur, G. M., and S. Solomon, *Aeronomy of the Middle Atmosphere*, 452 pp., D. Reidel, Norwell, Mass., 1986.

Brühl, C , S. R. Drayson, J. M. Russell III, P. J. Crutzen, J. M. McInerney, P. N. Purcell, H. Claude, H. Gernandt, T. J. McGee, I. S. McDermid, and M. R. Gunson, Halogen Occultation Experiment ozone channel validation, *J. Geophys. Res.*, *101*, 10,217-10,240, 1996.

Charney, J. G., and P. G. Drazin, Propagation of planetary scale disturbances from the lower into the upper atmosphere, *J. Geophys. Res.*, *66*, 83-109, 1961.

Chipperfield, M. P., Multiannual simulations with a three-dimensional chemical transport model, *J. Geophys. Res.*, *104*, 1781-1805, 1999.

Coy, L., and R. Swinbank, The characteristics of stratospheric winds and temperatures produced by data assimilation, *J. Geophys. Res.*, *102*, 25,763-25,781, 1997.

Dobson, G. M. B , A. W. Brewer, and B. M Cwilong, Meteorology of the lower stratosphere, *Proc. R. Soc. London, Ser. A*, *185*, 144-175, 1946.

Ehhalt, D. H., E. P. Roth, and U Schmidt, On the temporal variance of stratospheric trace gas concentrations, *J. Atmos. Chem.*, *1*, 27-51, 1983.

Eluszkiewicz, D., D. Crisp, R. G. Grainger, A. Lambert, A. E. Roche, J. B. Kumer, and J. L. Mergenthaler, Sensitivity of the residual circulation diagnosed from the UARS data to the uncertainties in the input fields and to the inclusion of aerosols, *J Atmos. Sci.*, *54*, 1739-1757, 1997.

Farman, J. C., R. J. Murgatroyd, A. M. Silnickas, and B. A. Thrush, Ozone photochemistry in the Antarctic stratosphere in summer, *Q. J R. Meteorol. Soc.*, *111*, 1013-1028, 1985.

Froidevaux, L., et al., Validation of UARS Microwave Limb Sounder ozone measurements, *J. Geophys. Res.*, *101*, 10,017-10,060, 1996.

Gao, R. S., et al., A comparison of observations and model simulations of NO_x/NO_y in the lower stratosphere, *Geophys Res. Lett.*, *26*, 1153-1156, 1999.

Gettelman, A., J. R. Holton, and K. H. Rosenlof, Mass fluxes of O_3, CH_4, N_2O and CF_2Cl_2 in the lower stratosphere calculated from observational data, *J. Geophys. Res.*, *102*, 19,149-19,159, 1997.

Hess, P. G., and J. R Holton, The origin of temporal variance in long-lived trace constituents in the summer stratosphere, *J. Atmos. Sci.*, *42*, 1455-1462, 1985.

Holton, J. R., and W. Choi, Transport circulation deduced from SAMS trace species data, *J. Atmos. Sci.*, *45*, 1929-1939, 1988.

Jackman, C. H., E. L. Fleming, S. Chandra, D. B. Considine, and J. E. Rosenfield, Past, present, and future modeled ozone trends with comparisons to observed trends, *J. Geophys. Res.*, *101*, 28,753-28,767, 1996.

Johnston, H. S., Global ozone balance in the natural stratosphere, *Rev Geophys.*, *13*, 637-649, 1975.

Krueger, A. J., The global distribution of total ozone: TOMS satellite measurements, *Planet. Space Sci.*, *37*, 1555-1565, 1989.

Lary, D. J., M. P. Chipperfield, J. A. Pyle, W A. Norton, and L. P. Riishojgaard, Three-dimensional tracer initialization and general diagnostics using equivalent PV latitude-potential-temperature coordinates, *Q. J. R. Meteorol. Soc.*, *121*, 187-210, 1995

Luo, M., J. H. Park, K. M. Lee, J. M. Russell III, and C. Brühl, An analysis of HALOE observations in summer high latitudes using airmass trajectory and photochemical model calculations, *J. Geophys Res* , *102*, 16,145-16,156, 1997.

Murgatroyd, R. J., and F. Singleton, Possible meridional circulations in the stratosphere and mesosphere. *Q. J. R. Meteorol. Soc.*, *87*, 125-135, 1961.

Natarajan, M. and L. B. Callis, Ozone variability in the high latitude summer stratosphere, *Geophys. Res. Lett.*, *24*, 1191-1194, 1997.

Newman, P. A., M. R. Schoeberl, R. A Plumb, and J. E. Rosenfield, Mixing rates calculated from potential vorticity, *J. Geophys. Res.*, *93*, 5221-5240, 1988.

Newman, P.A., D. W. Fahey, W. H. Brune, M. J. Kurylo, and S. R. Kawa, Preface, *J. Geophys Res.*, *104*, 26,481-26,495, 1999.

Park, J. H., and J. M. Russell III, Summer polar chemistry observations in the stratosphere made by HALOE, *J. Atmos. Sci.*, *51*, 2903-2913, 1994.

Park, J. H., et al., Validation of Halogen Occultation Experiment CH_4 measurements from the UARS, *J. Geophys. Res.*, *101*, 10,183-10,203, 1996.

Perliski, L. M., S. Solomon and J. London, On the interpretation of seasonal variations of stratospheric ozone, *Planet. Space Sci.*, *37*, 1527-1538, 1989.

Randel, W. J., Global Atmospheric Circulation Statistics, 1000-1 mb, *NCAR Tech. Note NCAR/TN-295+STR*, Natl. Cent. For Atmos. Res , Boulder, Colo., 1987.

Randel, W. J., and R. R. Garcia, Application of a planetary wave breaking parameterization to stratospheric circulation statistics, *J. Atmos. Sci* , *51*, 1157-1168, 1994.

Randel, W. J., F. Wu, J. M. Russell III, A. Roche, and J. W. Waters, Seasonal cycles and QBO variations in stratospheric CH_4 and H_2O observed in UARS HALOE data, *J. Atmos. Sci.*, *55*, 163-185, 1998

Roche, A. E., et al., Validation of CH_4 and N_2O measurements by the Cryogenic Limb Array Etalon Spectrometer instrument on the Upper Atmosphere Research Satellite, *J. Geophys. Res.*, *101*, 9679-9710, 1996.

Rosenfield, J. E., M. R. Schoeberl, and M. A. Geller, A computation of the stratospheric diabatic circulation using an accurate radiative transfer model, *J. Atmos. Sci.*, *44*, 859-876, 1987

Rosenfield, J. E., P. A. Newman, and M. R. Schoeberl, Computations of diabatic descent in the stratospheric polar vortex, *J. Geophys. Res.*, *99*, 16,677-16,689, 1994.

Rosenfield, J. E., D. B. Considine, P. E. Meade, J T. Bacmeister, C. H. Jackman and M. R. Schoeberl, Stratospheric effects of Mount Pinatubo aerosol studied with a coupled two-dimensional model, *J. Geophys. Res.*, *102*, 3649-3670, 1997.

Rosenlof, K H., Seasonal cycle of the residual mean meridional circulation in the stratosphere, *J. Geophys. Res.*, *100*, 5173-5191, 1995.

Rosenlof, K. H., Estimates of the seasonal cycle of mass and ozone transport at high northern latitudes, *J. Geophys. Res.*, *104*, 26,511-26,523, 1999.

Russell, J. M., III, et al., The Halogen Occultation Experiment, *J. Geophys. Res.*, *98*, 10,777-10,797, 1993.

Russell, J. M., III, et al., Validation of hydrogen fluoride measurements made by the Halogen Occultation Experiment from the UARS platform, *J. Geophys. Res.*, *101*, 10,163-10,174, 1996.

Sabutis, J. L, The short-term transport of zonal mean ozone using a residual mean circulation calculated from observations, *J. Atmos. Sci.*, *54*, 1094-1106, 1997.

Shine, K , Sources and sinks of zonal momentum in the middle atmosphere diagnosed using the diabatic circulation, *Q. J. R. Meteorol. Soc.*, *115*, 265-292, 1989.

Swinbank, R., and A. O'Neill, A stratosphere-troposphere data assimilation system, *Mon. Weather Rev.*, *122*, 686-702, 1994.

E. C Cordero, Department of Mathematics and Statistics, Monash University, Clayton, Victoria, 3168, Australia. (ecc@vortex.shm.monash.edu.au)

S. R. Kawa, Atmospheric Chemistry and Dynamics Branch, NASA Goddard Space Flight Center, Greenbelt, MD, 20771.

(Received August 29, 2000; revised January 3, 2001;
accepted January 5, 2001.)